How well do stomatal conductance models perform on closing plant carbon budgets? A test using seedlings grown under current and elevated air temperatures

Danielle A. Way,[1,2] Ram Oren,[1,3] Hyun-Seok Kim,[1,4] and Gabriel G. Katul[1,5]

Received 12 July 2011; revised 10 October 2011; accepted 14 October 2011; published 22 December 2011.

[1] Future carbon and water fluxes within terrestrial ecosystems will be determined by how stomatal conductance (g_s) responds to rising atmospheric CO_2 and air temperatures. While both short- and long-term CO_2 effects on g_s have been repeatedly studied, there are few studies on how g_s acclimates to higher air temperatures. Six g_s models were parameterized using leaf gas exchange data from black spruce (*Picea mariana*) seedlings grown from seed at ambient (22/16°C day/night) or elevated (30/24°C) air temperatures. Model performance was independently assessed by how well carbon gain from each model reproduced estimated carbon costs to close the seedlings' seasonal carbon budgets, a 'long-term' indicator of success. A model holding a constant intercellular to ambient CO_2 ratio and the Ball-Berry model (based on stomatal responses to relative humidity) could not close the carbon balance for either treatment, while the Jarvis-Oren model (based on stomatal responses to vapor pressure deficit, D) and a model assuming a constant g_s each closed the carbon balance for one treatment. Two models, both based on g_s responses to D, performed best overall, estimating carbon uptake within 10% of carbon costs for both treatments: the Leuning model and a linear optimization model that maximizes carbon gain per unit water loss. Since g_s responses in the optimization model are not a priori assumed, this approach can be used in modeling land-atmosphere exchange of CO_2 and water in future climates.

Citation: Way, D. A., R. Oren, H.-S. Kim, and G. G. Katul (2011), How well do stomatal conductance models perform on closing plant carbon budgets? A test using seedlings grown under current and elevated air temperatures, *J. Geophys. Res.*, *116*, G04031, doi:10.1029/2011JG001808.

1. Introduction

[2] Descriptions of stomatal responses to environmental drivers are needed when estimating the simultaneous exchange rates of heat, carbon dioxide, and water vapor between terrestrial ecosystems and the atmosphere [*Sellers et al.*, 1995, 1996; *Baldocchi and Meyers*, 1998; *Lai et al.*, 2000; *Siqueira and Katul*, 2002; *Juang et al.*, 2008]. Studies showing that rising atmospheric CO_2 reduces, or does not affect, leaf-scale stomatal conductance (g_s) are numerous, spanning over 100 years [*Darwin*, 1898; *Scarth*, 1927; *Meidner*, 1987; *Ellsworth et al.*, 1995; *Heath*, 1998; *Medlyn et al.*, 2001; *Schäfer et al.*, 2002; *Wullschleger et al.*, 2002; *Ainsworth and Rogers*, 2007; *Konrad et al.*, 2008]. More importantly, the implications of reductions in g_s with rising atmospheric CO_2 for global carbon and water cycles have been considered within the context of global climate models, suggesting increased continental scale runoff and a positive feedback on rising air temperatures [*Cox et al.*, 2000; *Gedney et al.*, 2006; *Betts et al.*, 2007].

[3] However, stomatal responses to another concomitant global change factor, rising air temperatures, are less certain. With increasing leaf temperatures, g_s can increase, decrease, show a peaked function, or remain relatively constant [*Kemp and Williams*, 1980; *Monson et al.*, 1982; *Sage and Sharkey*, 1987; *Santrucek and Sage*, 1996; *Cowling and Sage*, 1998; *Day*, 2000; *Yamori et al.*, 2006; *Weston and Bauerle*, 2007; *Kubien and Sage*, 2008; *Way and Sage*, 2008a, 2008b; *Mott and Peak*, 2010; *Silim et al.*, 2010], although this response is often complicated by responses of g_s to vapor pressure deficit (D) when D is not controlled during measurements. The mechanism driving stomatal sensitivity to short-term changes in leaf temperature is still a matter of debate [*Fredeen and Sage*, 1999; *Peak and Mott*, 2011; *Pieruschka et al.*, 2010]. But even if the short-term (minutes to hours) response of g_s to a change in leaf temperature was predictable, long-term acclimation to different growth temperatures can alter the response of stomata to leaf temperature. Plants

[1]Nicholas School of the Environment, Duke University, Durham, North Carolina, USA.
[2]Department of Biology, Duke University, Durham, North Carolina, USA.
[3]Department of Forest Ecology and Management, Swedish University of Agricultural Sciences, Umeå, Sweden.
[4]Department of Forest Sciences, College of Agriculture and Life Sciences, Seoul National University, Seoul, South Korea.
[5]Department of Civil and Environmental Engineering, Duke University, Durham, North Carolina, USA.

0148-0227/11/2011JG001808

grown at different thermal regimes often have a similar shape in the response of g_s to leaf temperature, although with differing values of g_s [*Kemp and Williams*, 1980; *Yamori et al.*, 2006]. However, leaves acclimated to different growth temperatures can show differing, or even opposite, patterns in how g_s responds to increasing leaf temperatures [*Santrucek and Sage*, 1996; *Way and Sage*, 2008a; *Silim et al.*, 2010]. While the precise pathways responsible for these differences in g_s values and g_s response patterns remains to be explored, elevated growth temperatures may alter plant allometry in a predictable way, with impacts on plant water use. *Way and Oren* [2010] found that elevated growth temperatures led to relative increases in leaf mass and relative reductions in root mass, which if not countered by other hydraulic adjustments could affect stomatal control by reducing the ability of trees to transport sufficient water to their leaves to match evaporative demand.

[4] Stomatal responses to changes in environmental variables, such as air temperature, are often predicted with a number of commonly used models [*Damour et al.*, 2010]. One type of model is a hydro-mechanical model that uses epidermal and whole-plant water relations and leaf biochemistry to estimate g_s [e.g., *Buckley et al.*, 2003]. A second category of models uses semi-empirical formulations to link g_s to environmental parameters [*Jarvis*, 1976] or linearly to the photosynthetic rate (A) [*Ball et al.*, 1987; *Collatz et al.*, 1991; *Leuning*, 1995]. These semi-empirical models are widely used in current climate, hydrologic, and ecosystem carbon models [*Sellers et al.*, 1995; *Baldocchi*, 1997; *Anderson et al.*, 2000; *Luo et al.*, 2001; *Whitehead et al.*, 2001; *Reichstein et al.*, 2003; *Blanken and Black*, 2004; *Keenan et al.*, 2010]. A third category assumes that stomata optimally and autonomously regulate their aperture to maximize carbon gain at a given water loss rate, without explicitly resolving the pathways and biochemical signaling mechanisms responsible for stomatal opening and closure [*Givnish and Vermeij*, 1976; *Cowan*, 1978; *Cowan and Farquhar*, 1977; *Hari et al.*, 1986]. Unlike semi-empirical models, the optimization approach does not a priori assume how g_s responds to environmental drivers from existing sets of data, but attempts to derive such responses based on an optimality hypothesis. This point may be especially important with climate change, as plants develop under conditions outside of their current range of air temperatures and CO_2 concentrations.

[5] While some of these stomatal models are widely used, studies evaluating their relative performances are uncommon, especially under future climate conditions. *Medlyn et al.* [2001] studied how two semi-empirical models performed on trees from ambient and elevated CO_2 concentrations, concluding that the sensitivity of g_s to environmental parameters (including D and CO_2) was unchanged by growth CO_2 in the Jarvis model, as was the relationship between g_s and photosynthesis in the Ball-Berry model. *Katul et al.* [2010] compared two semi-empirical models (the Ball-Berry and Leuning models) with an optimization approach on *Pinus taeda* grown at ambient and elevated CO_2 concentrations, and found that the optimization approach described the data at least as well as the semi-empirical models, provided the cost-of-water parameter linearly increased with increasing CO_2. Last, *Nijs et al.* [1997] compared semi-empirical models and a water-use-efficiency maximization approach for *Lolium perenne* grown at ambient conditions, elevated CO_2, elevated temperature, or both high CO_2 and temperature, and found that the Leuning model performed better than either the Ball-Berry model or the model that maximized instantaneous water use efficiency (WUE = photosynthesis/transpiration, A/E). The approach of both *Katul et al.* [2010] and *Nijs et al.* [1997] was to focus on instantaneous gas-exchange measurements (on the scale of minutes to an hour), comparing predictions and measurements of A, E, and intercellular CO_2 concentrations. However, evaluating the performance of these models over time-scales commensurate with changes in growth and carbon stocks (weeks to months) remains a challenge because of both endogenous (e.g., acclimation effects and leaf area development) and exogenous (e.g., large changes in environmental variables) effects. This evaluation requires confronting models with an extensive data set of both ecophysiological parameters and plant growth measurements to determine which model best predicts the carbon uptake necessary to close the carbon budget of the plant over a long period (e.g., months or longer). Because this suite of data is uncommon for one growth temperature, let alone for conditions similar to current and future climates, we are unaware of any attempts to compare existing g_s models using this approach.

[6] A data set on the growth and physiological parameters of black spruce (*Picea mariana* (Mill.) B.S.P.) is used here to compare the performance of six commonly used models for predicting g_s and A under ambient and elevated air temperature conditions. Data were derived from seedlings grown at either temperatures representing the species' current range or temperatures representing predicted boreal conditions for the year 2100 [*Way and Sage*, 2008a, 2008b]. The same measured photosynthetic and respiration parameters were used within a growth temperature to explore how well each g_s model predicted carbon uptake in plants grown under either current or warming conditions. Because gas exchange measurements were used to determine physiological parameters for the various models, model performance was judged by closure of the seedling carbon budget. Biomass changes occur on much longer time scales than the diurnal variations in meteorological drivers of g_s, making plant growth an appropriate scale to evaluate integrated long-term performance of such models. Unlike mature trees or ecosystems, in situ tracking of changes in biomass and carbon fluxes in seedlings can be quantified with relative ease and accuracy, making them an attractive system for exploring the potential of judging stomatal model performance on seasonal or other long-term timescales.

2. Methods

2.1. Data Description

[7] While much of the experimental setup is described elsewhere [*Way and Sage*, 2008a, 2008b], the salient features most pertinent to the g_s model calibration and evaluation are reviewed here. To model seasonal carbon gain and costs, data from two experiments where well watered black spruce seedlings were grown at either current or elevated growth temperatures were used [*Way and Sage*, 2008a, 2008b]. Seedlings were grown in greenhouses and growth chambers under ambient CO_2 concentrations (~380 ppm) at 22°C days

Table 1. Parameters, Parameter Values, and Temperature Correction Equations Used in Modeling Carbon Fluxes for Each g_s Model, Along With References for Those Values and Corrections[a]

		AT				HT				
Parameter (units)	Type	a	b	c	d	a	b	c	d	Data Source
V_{cmax} (μmol m^{-2} s^{-1})	Arr	33.0	58520			23.3	58520			Mean V_{cmax} at 25°C from *Way and Sage* [2008a, 2008b]; activation energy from *von Caemmerer and Quick* [2000]
K_c (μmol mol^{-1})	Arr	419	81655			419	81655			*Jordan and Ogren* [1981]; activation energies from *Jordan and Ogren* [1984]
K_o (mmol mol^{-1})	Arr	381	15632			381	15632			
$\Gamma*$ (μmol m^{-2} s^{-1})	poly	0.0021	0.1083	2.5821	9.8365	0.0012	0.0613	1.8469	14.348	*Yamori et al.* [2006]
R_{day} stem (gC m^{-2} d^{-1})	con	0.925				0.925				*Acosta et al.* [2008]
R_{dark} shoot (gC g^{-1} d^{-1})	Q_{10}	0.00454	2.2			0.00501	2.2			R_{dark} and assumed Q_{10} values, *Tjoelker et al.* [1999]
R_{dark} root (gC g^{-1} d^{-1})	Q_{10}	0.0245	2.2			0.0322	2.2			

[a]AT, ambient temperature treatment; HT, high temperature treatment; T_l, leaf temperature in °K. Equation types (type): Arrhenius (Arr): $y = ae^{[(T_l - 298)b]/(298 \times 8.314 \times T_l)}$; Polynomial (poly): $y = [a(T_l - 273)^3] - [b(T_l - 273)^2] + c(T_l - 273) + d$; Constant (con): $y = a$; Q_{10} equation (Q_{10}): $y = ab^{(-2/10)}$.

and either 14°C or 16°C nights (ambient temperature; AT) or 30°C days and either 22°C or 24°C nights (high temperature; HT). The data set for each treatment included about 1200 individual gas exchange measurements of g_s and A made at a range of light, CO_2, D and temperature conditions, measured with a portable photosynthesis device (Li-6400 and 6400–05, Li-cor Inc., Lincoln, Nebraska, USA). The data also included measurements of V_{cmax} (the maximum carboxylation efficiency of Rubisco), and the responses of V_{cmax} to changes in leaf temperature between 10°C and 40°C for each treatment. Table 1 summarizes the derived temperature response curve of V_{cmax} for each treatment. Growth trajectories for each treatment were also assessed, with shoot height, stem diameter, specific leaf area, and leaf, stem, and root biomass measured at multiple points over the growing season. Growth data from these two experiments were supplemented with height and biomass data from a set of black spruce seedlings simultaneously grown from seed in the same greenhouses as in the work by *Way and Sage* [2008a] but potted in fine gravel and frequently fertilized (D. A. Way and R. F. Sage, unpublished data, 2007).

2.2. Photosynthesis

[8] The basic leaf photosynthesis equation of the *Farquhar et al.* [1980] model can be expressed as:

$$A = a_1\left(\frac{C_i - \Gamma*}{a_2 + C_i}\right) \quad (1)$$

where A is the leaf biochemical demand for CO_2, a_1 and a_2 vary depending on whether A is Rubisco- or light-limited, C_i is the intercellular CO_2 concentration, and $\Gamma*$ is the CO_2 compensation point in the absence of mitochondrial respiration. When A is light-saturated, $a_1 = V_{cmax}$ and $a_2 = K_c\left(1 + \frac{O}{K_o}\right)$, where K_c and K_o are the Michaelis constants for carboxylation and oxygenation, and O is the ambient oxygen concentration. When A is light-limited, $a_1 = \alpha\phi_{max}Q$ and $a_2 = 2\Gamma*$, where α is the leaf light absorptivity (=0.8), ϕ_{max} is the maximum quantum efficiency (=0.08), and Q is the photosynthetic photon flux density (or PPFD). These α and ϕ_{max} values are standard taken from *Campbell and Norman* [1998]. The parameters $\Gamma*$, K_c and K_o were based on the same kinetics used to model black spruce by *Way and Sage* [2008b] and *Sage et al.* [2008] (Table 1) and O was set at 210 mmol mol^{-1}.

2.3. Gas Transport Between the Atmosphere and Leaves

[9] While equation (1) defines the biochemical demand for CO_2, the supply of CO_2 molecules transported from the atmosphere into the leaves can be expressed as a Fickian diffusion, given as:

$$A = g_s(C_a - C_i) = g_sC_a(1 - C_i/C_a) \quad (2)$$

where C_a is the atmospheric CO_2 concentration. Here, the leaf boundary layer and mesophyll resistances were neglected when compared to the stomatal resistance (=g_s^{-1}). The realized rate of photosynthesis is determined by the balance between the supply and demand functions (i.e., equations (1) and (2)). However, the two equations are not mathematically closed since g_s must be a priori known to solve for A and C_i, necessitating one additional equation. It is this 'closure' approximation and how it varies between ambient and elevated air temperature that is most uncertain and frames the compass of this work.

2.4. Stomatal Conductance Models and Their Parameterization

[10] By estimating g_s from the various models, their effects on A can be compared and these differences can be projected into seasonal carbon uptake to judge model performance. This approach was used to evaluate differences in predicted photosynthesis and seasonal carbon gain for six g_s (i.e., 'closure') models, presented in order of decreasing generality. For each model, the same measured photosynthetic parameters for equation (1) and respiration values for each treatment (Table 1) were used; thus, differences in carbon fixation between models are entirely due to differences in the closure model equation needed for predicting g_s, A and C_i.

Table 2. Comparison of Parameters and Parameter Values Used for Each g_s Model[a]

Parameter (units)	AT	HT
	Constant g_s	
g_s (mol m^{-2} s^{-1})	0.14	0.050
	Constant C_i/C_a	
C_i/C_a	0.70	0.70
	Ball-Berry	
m_1	2.851	8.099
b_1 (mol m^{-2} s^{-1})	0.0974	0.0336
	Leuning	
m_2	5.218	8.223
b_2 (mol m^{-2} s^{-1})	0.0565	0.0106
	Jarvis-Oren	
m_3	−1.4541	−3.0566
b_3 (mol m^{-2} s^{-1})	0.1532	0.2175
	Linear Optimization	
g_o (mol m^{-2} s^{-1})	0.061	0.038
s	0.70	0.70
λ (μmol mol^{-1})	$C_a(1\text{-}s)^2$	$C_a(1\text{-}s)^2$

[a]All data used to derive parameter values are from *Way and Sage* [2008a, 2008b], except for λ, which is derived from equation (9). AT, ambient temperature treatment; HT, high temperature treatment.

[11] The first model (Constant g_s) held a constant g_s, set for 0.14 and 0.05 mol m^{-2} s^{-1} for AT and HT spruce, respectively. By setting g_s to a constant value, equations (1) and (2) can now be solved for A and C_i. These two g_s values were determined from leaf gas-exchange, using the measured mean g_s for each group at leaf growth temperature, saturating light and ambient CO_2 concentrations (Table 2). The intent of 'fixing' these values of g_s to the long-term averages was simply to assess how important the precise diurnal variations of g_s are to the carbon balance of the seedlings beyond long-term mean daytime values. Upon setting g_s to a constant, A and C_i are given by:

$$A = \frac{1}{2}\left[a_1 + g_s(a_2 + C_a) + \sqrt{(-a_1 - g_s(a_2 + C_a))^2 - 4a_1 g_s(\Gamma_* + C_a)}\right];$$
$$C_i = C_a - \frac{A}{g_s}. \quad (3)$$

Note that a_1, a_2, and Γ_* do vary with temperature, that a_1 varies between AT and ET seedlings (V_{cmax} in Table 1) and that a_1 varies with light for low light levels. These variations were retained in equation (3).

[12] The second g_s model (Constant $C_i/C_a = s$ [*Norman*, 1982]) maintained a constant long-term ratio of intercellular CO_2 to atmospheric CO_2 concentrations of 0.7 (=s), regardless of changes in atmospheric evaporative demand. This value of s was determined from leaf-gas exchange measurements and was set to the mean daytime value measured for both AT and HT seedlings under the same environmental conditions as the Constant g_s model (Table 2). By setting s to a constant, equations (1) and (2) can now be solved to:

$$A = \frac{a_1(sC_a - \Gamma_*)}{a_2 + sC_a}; \quad g_s = \left(\frac{1}{1-s}\right)\frac{A}{C_a - \Gamma_*}. \quad (4)$$

It should be noted that this model maintains a saturating increase of A with C_a and preserves the linear relationship between g_s and $A/(C_a - \Gamma_*)$ in the models described next.

[13] The third model was the Ball-Berry model [*Ball et al.*, 1987] where stomata respond to relative humidity (RH) such that:

$$g_s = m_1 \frac{A}{C_a - \Gamma_*} RH + b_1, \quad (5)$$

while the fourth model was the Leuning model [*Leuning*, 1995], where stomata respond to D (instead of RH):

$$g_s = m_2 \frac{A}{C_a - \Gamma_*}\left(1 + \frac{D}{D_o}\right)^{-1} + b_2 \quad (6)$$

where m_1 and m_2 are species (or treatment) specific parameters, D_o is the sensitivity of g_s to D, and b_1 and b_2 are minimum g_s values. We determined b_1, b_2, m_1, and m_2 for both treatments by plotting measured g_s against either measured $\frac{A}{C_a - \Gamma_*} RH$ (for the Ball-Berry model) or measured $\frac{A}{C_a - \Gamma_*}\left(1 + \frac{D}{D_o}\right)^{-1}$ (for the Leuning model) and calculating the slopes (for m_1 and m_2) and intercepts (for b_1 and b_2) using standard least squares regression fitting for data, where PPFD was >400 μmol m^{-2} s^{-1} and CO_2 concentrations ranged from 300 to 500 μmol mol^{-1}, D/D_o = 0.6 for the Leuning model [*Oren et al.*, 1999] (Table 2). For each point in the Constant C_i/C_a, Ball-Berry and Leuning models, we temperature-corrected Γ_* (Table 1) to ensure no bias originated from this quantity, since Γ_* is temperature sensitive. Analytical solutions for A for the Ball-Berry and Leuning models can be found in the Appendix.

[14] The fifth model (Jarvis-Oren) was also based on 'prescribed' g_s responses to D, from AT and HT seedlings measured at near ambient CO_2 concentrations (300–500 μmol mol^{-1}) and PPFD values >400 μmol m^{-2} s^{-1}, consistent with the Ball-Berry and Leuning models [*Way and Sage*, 2008a, 2008b]. The approach of *Jarvis* [1976], as used by *Oren et al.* [1999], was employed to represent $g_s = g_{sref}(1 - m\ln D)$, where g_{sref} is g_s at a D of 1 kPa (reference D), where m was shown to be a near-constant across more than 60 species and varies between 0.5 to 0.6. Because the relationship between g_s and $\ln D$ varied with leaf temperature (Figures 1a and 1b), the data could not be readily described with a single function and the g_s measurements were binned into four temperature classes. Temperature classes were determined by binning leaf temperature data while excluding empty bins (e.g., there were no measurements between 12°C and 15°C), and separate g_s versus $\ln D$ relationships were fit for each leaf temperature class (Figures 1a and 1b). In each temperature class, g_s at a D of 1.6 kPa (the D used to model seasonal carbon gain; see below) was estimated using the modeled g_{sref} and slopes (Figures 1c and 1d). The final Jarvis-Oren model described the change in g_s at a D of 1.6 kPa with a change in leaf temperature for both treatments, and was in the form:

$$g_s = m_3(1/T_{leaf}) + b_3 \quad (7)$$

where m_3 is a treatment specific parameter, b_3 is a minimum g_s, and T_{leaf} is leaf temperature in °C (Table 2 and

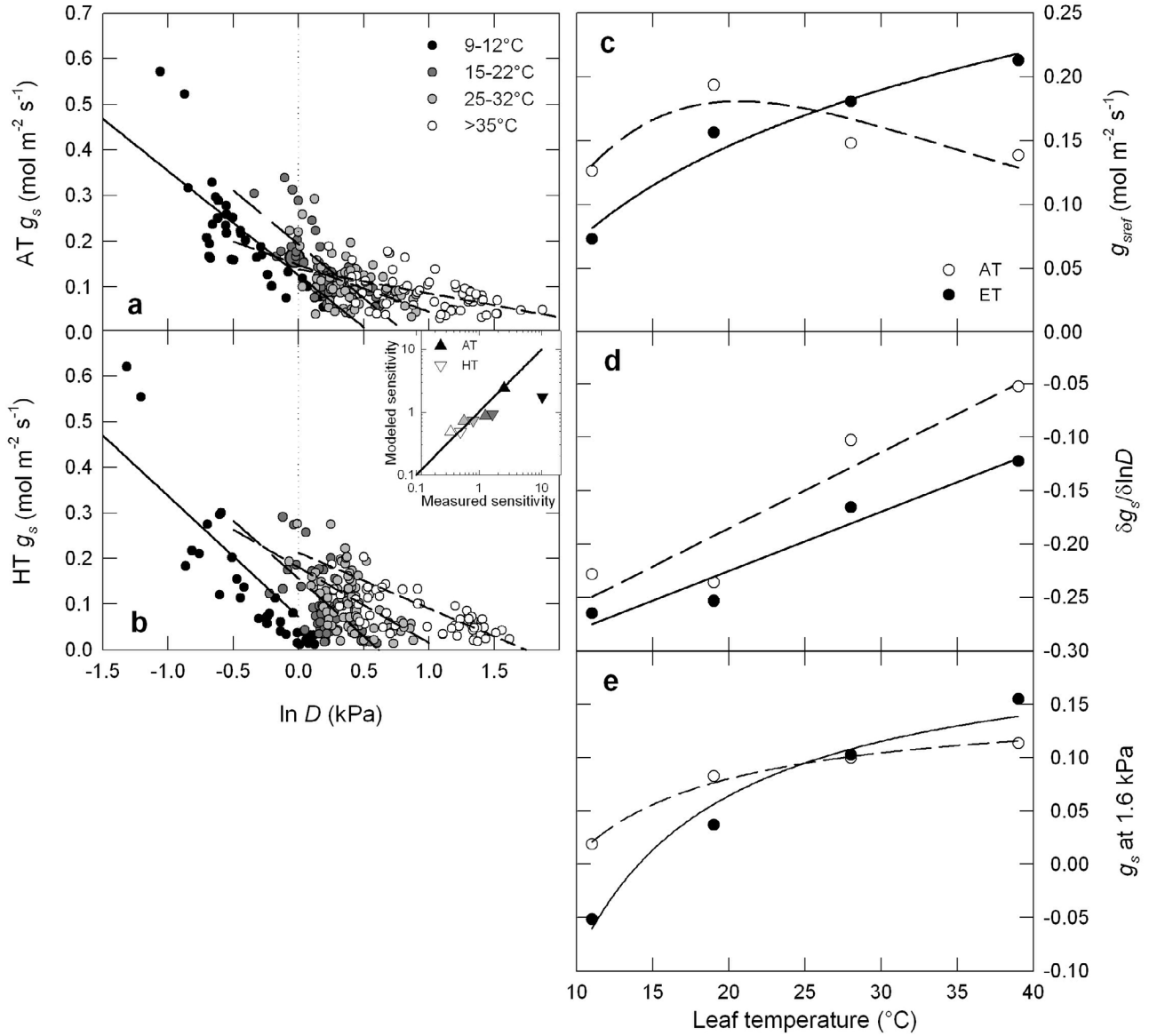

Figure 1. Response of stomatal conductance (g_s) to variation in vapor pressure deficit (D) measured at saturating light and different leaf temperature classes (symbols: 9°C–12°C, black; 15°C–22°C, dark gray; 25°C–32°C, light gray; >35°C, white) on black spruce grown at day/night temperatures of (a) 22/16°C (ambient temperature, AT) and (b) 30/24°C (high temperature, HT). Inset of Figure 1b compares the measured and modeled sensitivities (m_1/b_1) for each temperature class. Based on the relationships in Figures 1a and 1b, the effect of a change in leaf temperature on (c) g_{sref} (g_s at a reference D of 1 kPa); (d) $\delta g_s/\delta \ln D$; and (e) g_s at a D of 1 kPa (for b inset: AT, upward triangles; HT, downward triangle. For Figures 1c–1e: AT, open symbols, dashed lines; HT, filled symbols, solid lines).

Figure 1e). Equation (7) was used for the Jarvis-Oren model in the model comparison.

[15] Since there are expected relationships between $\delta g_s/\delta \ln D$ and g_{sref} in the Jarvis-Oren model [*Oren et al.*, 1999; *Kim et al.*, 2008], the expected sensitivity (defined as the ratio of $\delta g_s/\delta \ln D$ to g_{sref}) was modeled for the four temperature classes for each treatment as a test of the Jarvis-Oren model performance. Within each temperature class in each treatment, the relationship between g_{sref} and ln$D$ was determined using mean g_s values from each treatment, a boundary layer conductance (g_{bl}) of 0.936 mol m^{-2} s^{-1} to account for differences between needle and shoot boundary layers in black spruce [*Rayment et al.*, 2000], and all measurements where D was within two standard deviations of the mean D to exclude outliers from the D range data.

[16] The sixth model was a Linear Optimization model, based on the theory that g_s autonomously maximizes leaf carbon gain for a given water loss [*Givnish and Vermeij*, 1976; *Cowan*, 1978; *Cowan and Farquhar*, 1977; *Hari et al.*, 1986]. In linearizing the photosynthetic CO_2 curve of equation (1),

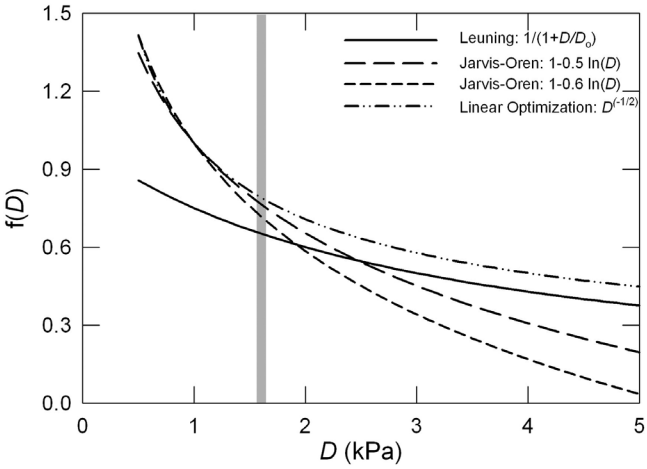

Figure 2. Effect of changes D on the functions relating g_s to D (f(D)) for the Leuning (solid line), Jarvis-Oren with m = 0.5 (long dashed line) or m = 0.6 (short dashed line), and Linear Optimization (dashed-dot line) models. Note that the Jarvis-Oren and Linear Optimization models define f(D) = 1 at D = 1 kPa. The gray box indicates a D of 1.6 kPa, the constant D used in the analysis.

Katul et al. [2009, 2010] derived analytical expressions for g_s, C_i/C_a and A that are here modified to account for Γ_* (see Appendix A):

$$g_s = \frac{a_1}{a_2 + sC_a}\left[-1 + \sqrt{\frac{(C_a - \Gamma_*)}{a\lambda D}}\right] + g_o \tag{8}$$

$$\frac{C_i}{C_a} = 1 - \sqrt{\frac{a\lambda D}{C_a}\left(\frac{C_a - \Gamma_*}{C_a}\right)} \tag{9}$$

$$A = \frac{a_1(C_a - \Gamma_*)}{a_2 + sC_a}\left[1 - \sqrt{\frac{a\lambda D}{(C_a - \Gamma_*)}}\right] \tag{10}$$

where s is, as before, the long-term mean C_i/C_a, a is the relative diffusivity of water compared to CO_2 (=1.6), g_o is nighttime stomatal conductance, and λ is a species-specific cost parameter for water loss in units of carbon (also known as the marginal water use efficiency, where $\lambda = \delta A/\delta E$). We set s to 0.7 based on the measured mean daytime C_i/C_a for both AT and HT seedlings measured at daytime growth conditions (see Constant C_i/C_a model) and used the mean g_s measured in the dark at ambient CO_2 concentrations, and at temperatures within ±6°C of nighttime growth temperatures for each treatment to estimate g_o. Our value for λ was derived by rearranging equation (9) and assuming that $\frac{C_a - \Gamma_*}{C_a} \approx 1$, such that λ scales linearly with C_a (Table 2), consistent with the studies discussed by *Katul et al.* [2010] and *Manzoni et al.* [2011].

[17] The models, while different, have a number of underlying similarities. Operationally, the Linear Optimization model approximately retains the D response from *Oren et al.* [1999] used in the Jarvis-Oren model [*Katul et al.*, 2009]. The Linear Optimization model also retains the quasi-linear correlation between g_s and $A/(C_a\text{-}\Gamma_*)$ noted in the numerous gas exchange data sets used to derive the Ball-Berry and Leuning models, such that this relationship can be seen as an 'emergent' property of the Linear Optimization model, provided λ increases linearly with atmospheric CO_2 (as shown by *Katul et al.* [2009, 2010]). As well, the Leuning and Linear Optimization models only differ in their nonlinear functional dependence on D, which is most amplified for $D < D_o$, where the D reduction in the Leuning model is quasi-linear, but that of the Linear Optimization model exhibits significant nonlinearity (Figure 2; see Appendix A). Equation (9) from the Linear Optimization model is also consistent with studies showing that C_i/C_a decreases nonlinearly with increasing D [*Wong and Dunin*, 1987; *Mortazavi et al.*, 2005], which differs from the linear decline in C_i/C_a predicted by the Leuning model [*Katul et al.*, 2000].

2.5. Testing the Stomatal Conductance Models With the Carbon Budget Closure

[18] The total seedling biomass (B) evolves as:

$$\frac{dB}{dt} = CF[LA(t) \times A(t)] - (R_E + R_C); \tag{11}$$

which can be re-arranged to yield:

$$B(t_f) - B(t_i) = \int_{t_i}^{t_f} \{CF[LA(t) \times A(t)] - (R_E + R_C)\}dt; \tag{12}$$

where t is time, t_i, t_f are the beginning and end times of the growing season, CF is a conversion factor needed to convert CO_2 molecules to biomass carbon, LA is the total seedling leaf area (which evolves over time), R_E is autotrophic respiration, and R_C is the construction cost.

[19] With regards to modeling $A(t)$, diurnal leaf responses of g_s, C_i/C_a and net CO_2 flux rates were modeled for a

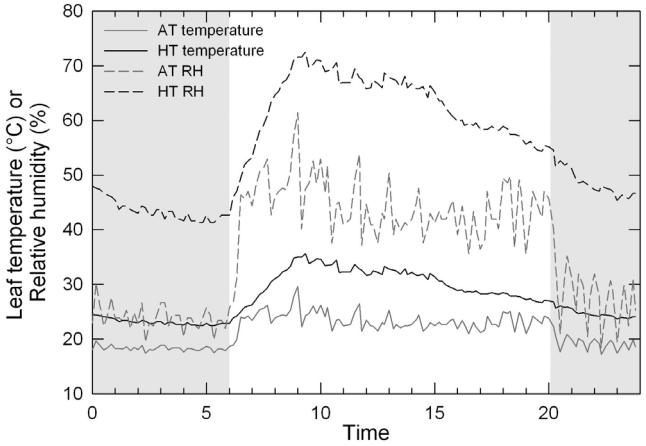

Figure 3. Measured leaf temperatures (solid lines) and calculated relative humidity based on constant D = 1.6 kPa (dashed lines) over the modeled 24 h period for black spruce grown at day/night temperatures of 22/16°C (ambient temperature, AT, gray lines) and 30/24°C (high temperature, HT, black lines). Shaded areas represent night in the photoperiod schedule.

24 h period with temperature and light conditions representative of the growth conditions in the work by *Way and Sage* [2008b]: mean leaf temperatures based on 24 h thermocouple readings, 14/10 day/night photoperiods, 800 μmol photons m^{-2} s^{-1} PPFD, 400 μmol mol^{-1} CO_2, and a constant D of 1.6 kPa (Figure 3). For the Constant g_s model, g_s was set and equations (1) and (2) were solved for A and C_i. For the Constant C_i/C_a model, we set C_i/C_a to its measured mean value and used equations (1) and (2) to predict A. For the Ball-Berry, Jarvis-Oren, Leuning, and Linear Optimization models, g_s, C_i, and A were solved based on equations (1) and (2) and the g_s equation for each of the four models. Net CO_2 assimilation rates (A_{net}) per unit leaf area were calculated for 10 min blocks using temperature-corrected V_{cmax} and Γ_* (Table 1). These rates were then converted to net carbon exchange (g C m^{-2}) for each 10 min interval of the light period and summed for a 24 h period for each g_s model.

[20] With regard to estimating $B(t_i)$, $B(t_f)$, and $LA(t)$, data on seedling growth were taken from AT and HT black spruce [*Way and Sage*, 2008a, 2008b]. *P. mariana* seeds are small (thousand-seed mass = 1.12 g [*Wang and Berjak*, 2000]), so $B(t_i)$ was ignored. Measured changes in leaf, stem, and root mass for each treatment were used to fit exponential growth trajectories for each pool over a 205 day timeframe (the duration of the experiment in the work by *Way and Sage* [2008b]), allowing us to estimate seasonal growth in each carbon pool, as well as total biomass (B). Using this 205 day growth season, the time evolution of LA in equation (12) was computed by converting calculated daily leaf mass for each treatment to daily leaf area, using measured specific leaf areas for each treatment. As in equation (12), the computed daily leaf area was multiplied by the modeled net carbon exchange per unit leaf area (in g C m^{-2}) for each g_s model to calculate daily carbon gain (in g C). Daily carbon gain values over the 205 days were then summed to obtain total leaf carbon gain over the growth season for each g_s model in each temperature treatment.

[21] The R_E was estimated from calculated daily leaf, stem, and root masses as above, as well as daily stem height and diameters calculated from exponential fits to measured changes in height and diameter for each treatment. Root respiration was calculated as daily root mass multiplied by root respiration rates from black spruce seedlings grown at either 24/18°C or 30/24°C day/night temperatures [*Tjoelker et al.*, 1999] over a 24 h period. Shoot dark respiration was calculated by using daily leaf and stem mass regressions, and shoot dark respiration rates for black spruce seedlings grown at either 24/18°C or 30/24°C day/night temperatures [*Tjoelker et al.*, 1999] over the night period, scaled to measured leaf temperatures with Q_{10} values from the same study. Published daytime stem respiration rates were on a surface area basis [*Acosta et al.*, 2008]. Hence, daily stem surface area was estimated using the regressions for shoot height and stem diameter and multiplying height by 2/3 diameter to account for stem taper. Because gas exchange was measured on branches and not just leaves, branch and leaf day respiration are already accounted for in values of A_{net}.

[22] To estimate carbon in live biomass at t_f (B_C), leaf, stem, and root mass values for day 205 were multiplied by measured %C values for leaves (47%) or values from the literature for stems (48% [*Iivonen et al.*, 2006; *Kaakinen et al.*, 2009; *Kostiainen et al.*, 2009]) and fine roots (45% [*Iivonen et al.*, 2006; *Jackson et al.*, 2009]). Construction costs of biomass (R_c) were estimated as 1.5 g glucose g^{-1} dry mass [*Niinemets*, 1997].

[23] Total seasonal carbon gain from each g_s model was compared to the summed carbon costs of biomass, construction costs, and respiration as $(C_{gains} - C_{costs})/C_{costs}$ to estimate closure of the seedlings' carbon budgets for each growth temperature, where:

$$C_{costs} = B_C + R_C(t_f) + \int_{t_i}^{t_f} \{R_E(t)\}dt;$$
$$C_{gains} = B(t_i) + \int_{t_i}^{t_f} \{CF[LA(t) \times A(t)]\}dt. \quad (13)$$

While the daily leaf area used to drive seasonal carbon gain was derived from regressions of leaf mass measurements (and seasonal specific leaf area), carbon costs relied on end of season total biomass, with leaf mass only contributing to carbon costs through the daily shoot mass regressions used to calculate shoot dark respiration.

[24] Because seasonal carbon costs were our benchmark for model performance, we estimated potential error in these costs by determining the minimum and maximum seasonal carbon costs from our measured biomass and measured and literature-based respiration rates. Although the modeled growing season was 205 days long, seedling biomass was measured for three independent replicates of the temperature acclimation experiment 197, 205 and 210 days after germination [*Way and Sage* 2008a, 2008b, unpublished data, 2007]. For each growth temperature, the smallest, youngest seedlings (197 days old) were used to estimate the lower value of mean seasonal biomass; the biggest, oldest seedlings (210 days old) were used to generate an upper value of seasonal biomass. Construction costs for these lower and upper bounds of seedling mass were determined as above. Since construction costs were based on biomass, biomass values accounted for 61%–79% of the minimum and maximum seasonal carbon cost estimates. Potential errors in respiratory costs were accounted for by using minimum and maximum estimates from the literature for stem day respiration [*Acosta et al.*, 2008] and the lowest and highest shoot dark respiration rates measured; root respiration was not varied, but accounted for <10% of total seasonal carbon costs. These lowest respiration costs were summed with the smallest seasonal biomass and construction costs to provide a minimum seasonal carbon cost estimate; the highest respiration rates were combined with the largest biomass and construction costs to generate an upper estimate of seasonal carbon costs. However, the estimates will inherently overestimate error in our modeled seasonal carbon costs. While all of the biomass measurements represent "end of season" biomass, plant growth is exponential; seedlings harvested 197 days after germination will be smaller than if they had grown for 205 days (the growth season modeled here), while the mass of seedlings grown for 210 days will be much greater than for those same seedlings 205 days after germination. Because these error estimates will be high, we also used a second, more conservative indicator of model success, by

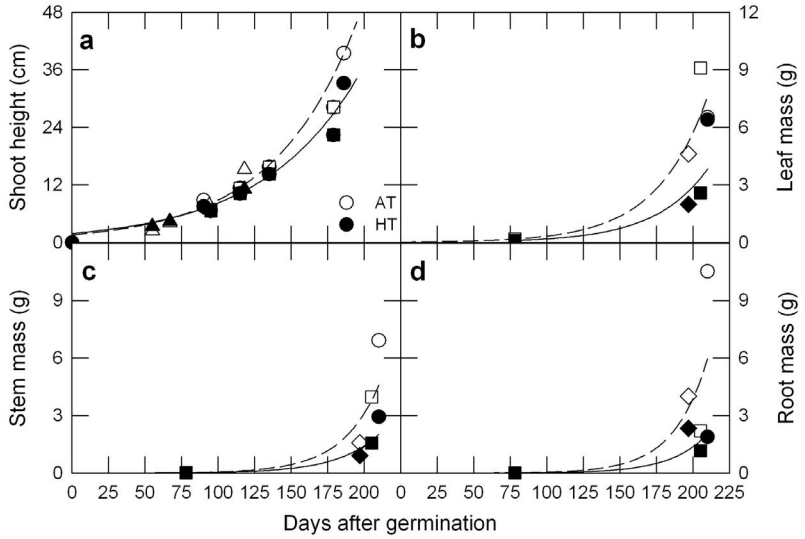

Figure 4. Growth of black spruce seedlings grown at 22/16°C (AT, open symbols, dashed lines) or 30/24°C (HT, filled symbols, solid lines) day/night temperatures. Circles and triangles, data from 2005 and 2006, respectively, from *Way and Sage* [2008a]; squares, data from *Way and Sage* [2008b]; diamonds, data from *Way and Sage* (unpublished data, 2007). (a) Shoot height, (b) leaf mass, (c) stem mass, and (d) root mass.

testing which g_s models generated seasonal carbon gain values within 10% of the modeled seasonal carbon losses.

2.6. Statistics

[25] Regressions and ANOVAs were performed in JMP 8.0.2 (SAS, Cary, North Carolina, USA).

3. Results

[26] The rate of seedling growth over time was consistent between experiments [*Way and Sage*, 2008a, 2008b, unpublished data, 2007], despite differences in maximum light levels and humidity conditions during growth, caused by greenhouse versus growth chamber growth conditions (Figure 4). Because seedling growth is exponential and the height and biomass data were best described, and described well, by exponential functions, we used exponential regressions to estimate seedling growth and mass. The most extensively measured parameter was shoot height, which was well-described with a single exponential growth function for each temperature treatment, with coefficients of determination (r^2) of 0.85 to 0.90 for AT and HT seedlings, respectively ($p < 0.0001$ for both; Figure 4a). Total biomass, leaf mass, stem mass, and root mass in each treatment also developed along similar exponential growth trajectories over time between experiments, with r^2 values ranging from 0.91 to 0.99 ($p < 0.022$ for all, Figures 4b–4d).

[27] The Constant C_i/C_a, Ball-Berry, and Leuning models and the Linear Optimization model's D reduction function all produced highly significant fits between the functions used to model g_s and the measured g_s values, and all provided a better fit to the HT data set (Figure 5). Coefficients of determination (r^2) for the AT and HT data, respectively, across the models were: Constant C_i/C_a, 0.04 ($p = 0.0013$) and 0.25 ($p < 0.0001$; Figure 5a); Ball-Berry, 0.04 ($p = 0.0019$) and 0.30 ($p < 0.0001$; Figure 5b); Leuning, 0.28 and 0.48 ($p < 0.0001$ for both; Figure 5c); and Linear Optimization D function, 0.24 and 0.49 ($p < 0.0001$ for both; Figure 5d). Growth at elevated temperatures increased m_1 and m_2 in the Ball-Berry and Leuning models, respectively (Table 2).

[28] In building the final Jarvis-Oren model equation, the relationship between g_s and ln$D$ was related to leaf temperature in both treatments (r^2 s of 0.22–0.73, $p < 0.0001$ for all; Figures 1a and 1b). While higher measurement temperatures often corresponded to higher D, within each temperature class, g_s was measured over a range of D and there was no pattern between temperature and D (data not shown). The measured sensitivity (i.e., the ratio of $\delta g_s/\delta \ln D$ to g_{sref}) of the AT data in each temperature class was consistent with the sensitivity modeled using the approach of *Oren et al.* [1999] (Figure 1b inset). However, the measured HT sensitivity deviated from modeled expectations at low leaf temperatures; there was good agreement between measured and modeled values at 30°C and 40°C, but measured sensitivity was slightly higher than expected at 20°C and much higher than predicted at 10°C leaf temperatures (Figure 1b inset). Values for g_{sref} increased with rising leaf temperatures in the HT treatment ($r^2 = 0.99$, $p < 0.005$), and peaked at moderate leaf temperatures (~20°C) for AT seedlings (Figure 1c); because the response of AT g_{sref} to temperature could not be significantly described for the four data points ($p > 0.05$), we selected the curve fit to both maximize the coefficients of determination and minimize the number of parameters ($r^2 = 0.74$, parameter n = 3). The slope of the relationship between g_s and ln$D$ increased with leaf temperature for both treatments, such that g_s was more sensitive to variation in D at low leaf temperatures than at warm temperatures ($r^2 = 0.88$–0.94, $p = 0.03$–0.06; Figure 1d). Values of g_s at a D of 1.6 kPa showed a similar response to rising leaf temperatures in both treatments ($r^2 = 0.97$–0.99, $p < 0.016$ for both; Figure 1e).

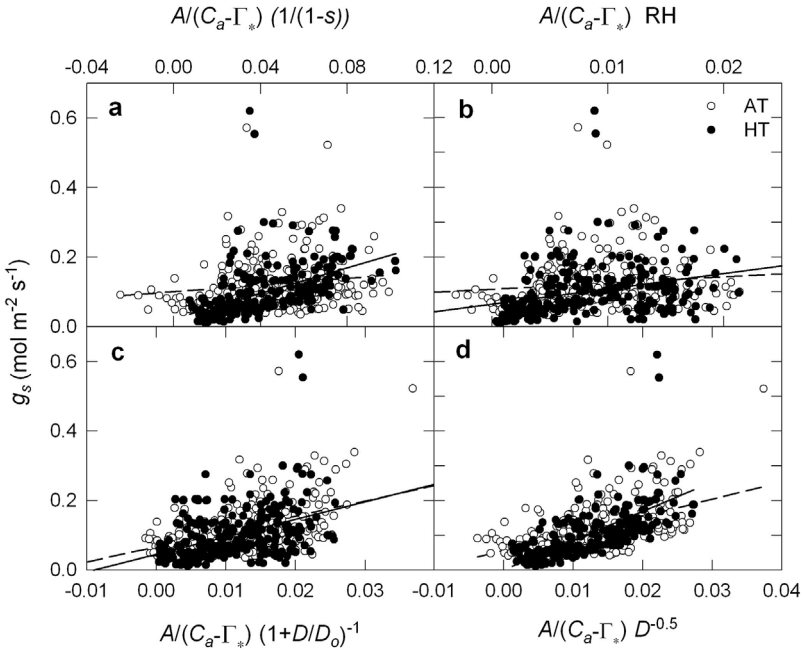

Figure 5. Response of measured stomatal conductance (g_s) to variation in: (a) the long-term mean ratio of intercellular to ambient CO_2 (s) for the constant C_i/C_a model; (b) relative humidity (RH), for the Ball-Berry model; or vapor pressure deficit (D), for the (c) Leuning and (d) Linear Optimization models, in combination with CO_2 assimilation (A), the CO_2 compensation point without mitochondrial respiration (Γ_*), and ambient CO_2 concentration (C_a). Data are from black spruce grown at day/night temperatures of 22/16°C (ambient temperature, AT, open symbols, dashed lines) and 30/24°C (high temperature, HT, filled symbols, solid lines).

[29] Daily courses of modeled g_s, C_i/C_a, A_{net} and carbon gain for each treatment varied considerably between models (Figure 6). For AT seedlings, the Constant C_i/C_a and Leuning models predicted the highest daytime g_s, while the Ball-Berry, Linear Optimization, and Jarvis-Oren models had similar, lower g_s values (Figure 6a). While the Leuning model also predicted relatively high g_s for the HT seedlings, the Jarvis-Oren model generated the highest g_s values, and although the Constant C_i/C_a model predicted high g_s in the AT treatment, it generated the lowest g_s values in the HT treatment (Figure 6b). In both the AT and HT scenarios, the Linear Optimization model consistently predicted the highest rates of net photosynthesis and daily carbon gain (Figures 6e–6h). Although there were not many gas exchange measurements at the modeled daytime conditions, model outputs can be compared to a subset of the data (n = 45 for AT and 15 for HT leaves) collected at saturating light, ambient CO_2 and leaf temperatures near growth conditions (25.2 ± 0.2°C for AT leaves and 35.3 ± 0.1°C for HT leaves, means ± SE). In this data set, A_{net} was 7.5 ± 0.3 for AT and 4.8 ± 0.4 μmol m^{-2} s^{-1} for HT seedlings, while g_s was 0.11 ± 0.01 and 0.09 ± 0.01 mol m^{-2} s^{-1} for AT and HT leaves, respectively (means ± SE). These measured g_s values were similar to model outputs for both treatments, with models predicting both higher and lower g_s, while the measured A_{net} values were slightly lower than modeled A_{net} for AT leaves and similar to the lower values modeled in the HT leaves by the Ball-Berry model (Figure 6). The mean daily WUE (A/E) predicted by each model was also compared between models, to determine whether models were generating realistic combinations of g_s and A_{net}. Values for modeled WUE at a D of 1.6 kPa ranged from 3.8–6.4 μmol CO_2/mmol H_2O in AT leaves and 2.8–10.7 μmol CO_2/mmol H_2O in HT leaves (Table 3); mean values for the subset of measured data near growth conditions and D near 1.6 kPa were 5.4 and 3.3 μmol CO_2/mmol H_2O for AT and HT spruce, with values ranging from 2.1–10.4 μmol CO_2/mmol H_2O.

[30] Modeled seasonal carbon costs for a 205 day growing season (based on exponential biomass growth, respiration, and construction costs as described above) were in the middle of the range of seasonal carbon costs estimated from total biomass harvested 197 and 210 days after germination, along with minimum and maximum respiration estimates. Estimates of carbon costs based on 197 day old seedlings were 35% lower than modeled 205 day carbon costs, while maximum seasonal carbon cost estimates from 210 day old seedlings ranged from 28%–35% greater than modeled carbon costs (Figure 7a). Since exponential growth produces rapid changes in total mass (Figure 7a inset), the actual seasonal carbon costs for seedlings that are 205 days old (as modeled here) will be larger than those estimated from seedlings that were harvested 197 days after germination and will be smaller than those derived from seedlings that are five days older (210 days old). Because our estimates of minimum and maximum seasonal carbon gain from measured seedlings were expected to be overestimates, we also used our modeled carbon costs with a 10% error as a more stringent estimate of the ability of the g_s models to describe the carbon gain of both treatments (Figure 7b).

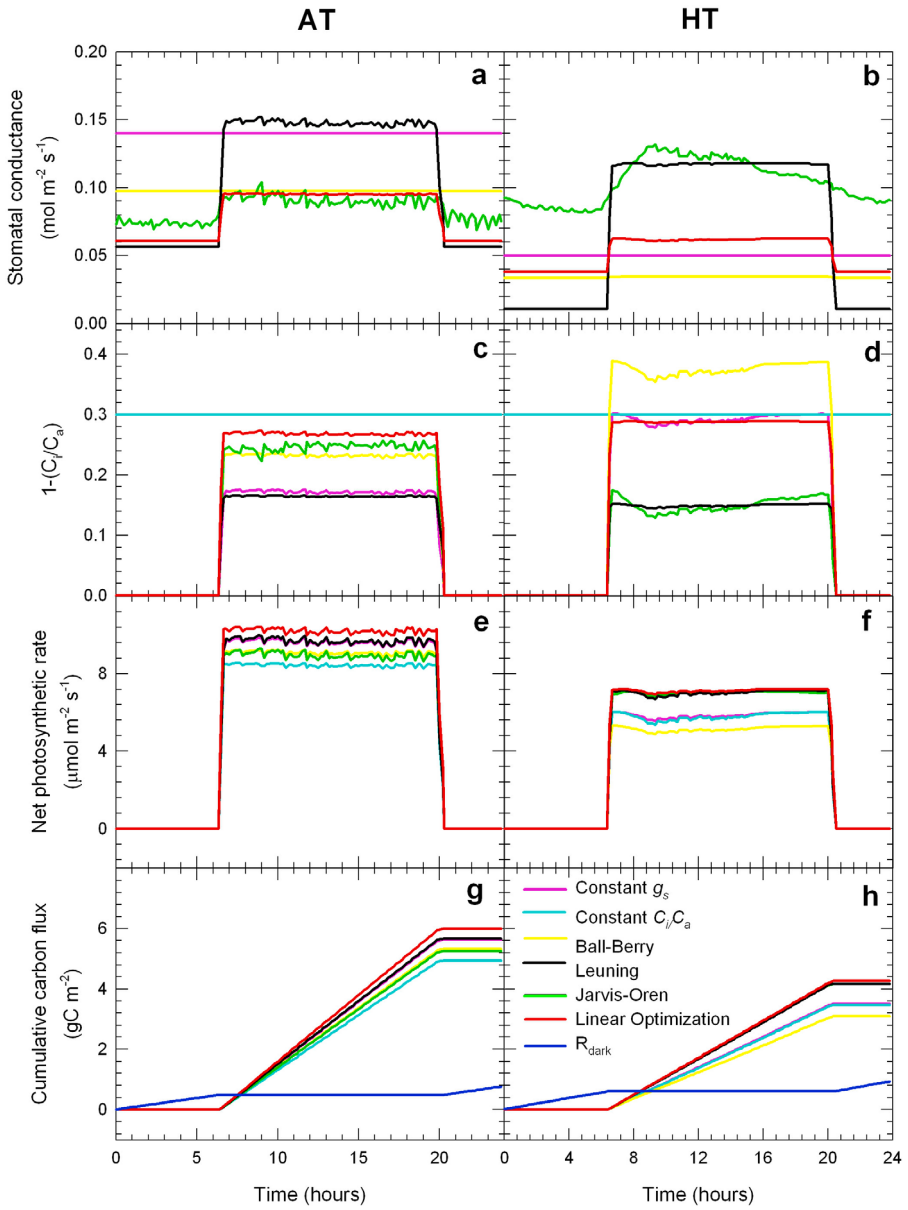

Figure 6. Diurnal time course of (a, b) stomatal conductance (g_s), (c, d) 1 minus the ratio of intercellular to ambient CO_2 (C_i/C_a), (e, f) net CO_2 assimilation rates (A_{net}), and (g, h) carbon gain (or loss, for dark respiration) for various g_s models for black spruce grown at 22/16°C (ambient temperature; AT) or 30/24°C day/night temperatures (high temperature; HT, black circles). Models: Constant g_s (magenta); Constant C_i/C_a (cyan); Ball-Berry (yellow); Leuning (black); Jarvis-Oren (green); Linear Optimization (red); dark respiration (R_{dark}, blue). Note that there are no g_s estimates for the Constant C_i/C_a model in Figures 6a and 6b.

[31] Models varied considerably in their ability to estimate the carbon gain necessary to match the seasonal carbon costs and in the consistency of their performance between the growth temperatures (Figures 7a and 7b). All of the models were able to predict a sufficiently high carbon gain to match the minimum seasonal carbon costs estimated from each treatment (i.e., that of 197 day old seedlings; Figure 7a). However, only the Leuning and Linear Optimization models successfully described the carbon budget of both treatments within 10% of the best estimate of total carbon costs for 205 day old seedlings (Figure 7b). The Constant g_s and Jarvis-Oren models could predict the carbon gain of either

Table 3. Comparison of Mean Daily Instantaneous Water Use Efficiencies for Each g_s Model[a]

Model	AT (±SD)	HT (±SD)
Constant g_s	4.3 ± 1.7	7.4 ± 0.2
Ball-Berry	5.5 ± 2.0	10.7 ± 0.3
Jarvis-Oren	6.3 ± 0.4	2.8 ± 0.3
Leuning	3.8 ± 1.0	3.8 ± 0.1
Linear Optimization	6.4 ± 1.1	7.2 ± 0.1

[a]WUE measured in μmol CO_2/mmol H_2O. AT, ambient temperature treatment; HT, high temperature treatment.

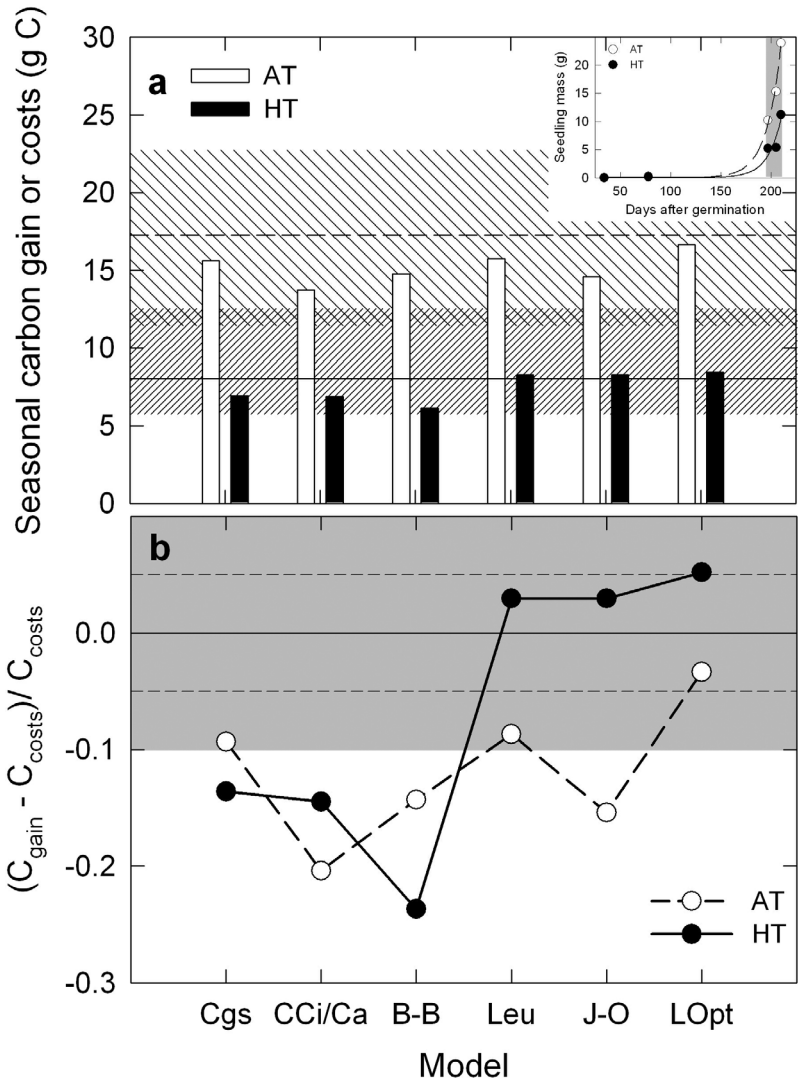

Figure 7. (a) Estimated seasonal carbon gain of g_s models for black spruce grown at 22/16°C (AT, white bars) or 30/24°C (HT, black bars) day/night temperatures. Estimated seasonal carbon costs for AT (horizontal dashed line) and HT seedlings (horizontal solid line) grown for 205 days; hatched boxes indicate range of end of season carbon costs for AT (coarse hatching) and HT seedlings (fine hatching) for seedlings harvested between 197 or 210 days after germination (minimum and maximum seasonal carbon cost estimates, respectively). Inset shows biomass growth of AT (empty circles, dashed lines) and HT seedlings (filled circles, solid lines), with the gray box indicating growth between 197 and 210 days after germination; (b) success of stomatal models in closing the carbon budget of AT (empty circles, dashed lines) or HT seedlings (filled circles, solid lines); gray box represents 10% from closure, dashed lines represent 5% from closure. Models: Cgs, constant g_s; CCi/Ca, constant C_i/C_a; B-B, Ball-Berry; Leu, Leuning; J-O, Jarvis-Oren; LOpt, linear optimization.

the AT or HT seedlings, respectively, for this more stringent criterion, but could not equally estimate seedling carbon gain for the second treatment (Figure 7b). In contrast, the Constant C_i/C_a and Ball-Berry models were unsuccessful in capturing the carbon fluxes for either group of trees within 10% of modeled carbon costs.

4. Discussion

[32] Seasonal carbon costs were used as the benchmark for g_s model performance, and since carbon costs were mainly determined by biomass (directly and also indirectly through construction costs), we assessed potential error in our biomass values by using measured seedling mass at the end of the growing season in three different replicate experiments. While this produced a twofold range of values that encompassed our modeled carbon cost values (Figure 7a), this is certainly an overestimate of the uncertainty of these measurements. The minimum carbon cost was estimated from plants harvested eight days earlier than our modeled growing season length of 205 days, and would be higher with an extra week of exponential growth. Similarly, the maximum estimated carbon costs were derived from seedlings harvested five days later than our 205 day modeled growing season

length and thus overestimate seasonal growth and carbon costs.

[33] Since it is implausible to collect measurements of g_s responses to environmental variation for all species of interest, models of g_s are needed. One way to judge model performance is to compare measured versus modeled g_s, as shown in Figure 5. However, our interest was in whether g_s models could be tested on a longer time scale. Of the six g_s models tested here, only the Leuning and Linear Optimization models captured the carbon gain for both treatments within 10% of our carbon loss values. The Constant g_s model met the 10% threshold criteria for AT seedlings and the Jarvis-Oren model for HT seedlings, while the Constant C_i/C_a and Ball-Berry models underestimated carbon gain in both treatments by more than 10%, with the Ball-Berry model underestimating carbon gain by more than 20% for the HT data. Contrasting the results between the g_s models and treatments allows us to narrow down the reasons for the variation in long-term model performance.

[34] Neither the Constant g_s model nor the Constant C_i/C_a model performed very well in closing the carbon budgets, although the Constant g_s model predicted carbon gain just within 10% of estimated carbon costs for AT seedlings. While conifer stomata tend to be slow to respond to changes in their environment, thus dampening the extent of their response to stimuli [*Watts and Neilson*, 1978; *Ng and Jarvis*, 1980], these responses must still be included in models to fully capture the plant's carbon dynamics. As well, spruce from both the AT and HT treatments had a similar mean C_i/C_a of 0.7, implying that this might represent an optimal balance between g_s and A_{net} across growth temperatures [*Wong et al.*, 1979]. However, the Constant C_i/C_a model could not satisfactorily predict carbon gain in either treatment, thereby disputing the idea of an optimal C_i/C_a.

[35] The Ball-Berry and Leuning models have similar forms, but the Ball-Berry model predicts g_s based on RH responses and the Leuning model from responses to D (compare equations (4) and (5)). While the Leuning model described both AT and HT carbon gain well, the Ball-Berry model performed poorly with both sets of data, due to its predictions of very low g_s. Given the low explanatory power of the Ball-Berry model on the g_s data (Figure 5b), its inability to predict g_s, and thus carbon gain, is not surprising. However, the differences in the carbon balance predictions between the Ball-Berry and Leuning models also imply that D is a better predictor of g_s than relative humidity, a result with empirical support in the physiological literature [*Aphalo and Jarvis*, 1991] and in a previous comparison of the Ball-Berry and Leuning models on plants grown at elevated temperatures [*Nijs et al.*, 1997]. Indeed, the models that performed best overall in our analysis (Leuning, Linear Optimization as well as the Jarvis-Oren model for HT seedlings), all related g_s to D. While the conceptual linkage of g_s to D is similar in the three models, the forms of the relationship are different, with important implications for predicting g_s as D rises (Figure 2). At low D (<1 kPa), the Linear Optimization model and the function used in the Jarvis-Oren model [from *Oren et al.*, 1999] are similar, but contrast with the Leuning model. When D is high (>3 kPa), the Leuning and Linear Optimization formulations become quasi-linear, while the *Oren et al.* [1999] function continues to decline. The distinctions between these models, especially at high D, will be important in a warming world, since climate warming is not expected to significantly alter air relative humidity, but should increase D because of increases in saturation vapor pressure [*Kumagai et al.*, 2004].

[36] There was good agreement between the measured and expected sensitivities (the ratio of $\delta g_s/\delta \ln D$ to g_{sref}) of the Jarvis-Oren model in AT seedlings in all temperature classes and for HT seedlings measured at moderate to high leaf temperatures, demonstrating that this data was well-described by the relationships derived by *Oren et al.* [1999]. However, HT sensitivity was much higher than expected at leaf temperatures near 10°C. While the AT data was captured within each temperature class by the Jarvis-Oren model, the pattern of responses of g_{sref} and $\delta g_s/\delta \ln D$ to leaf temperature in the AT treatment were less reasonable. The estimation of AT daily carbon gain operated in the range of leaf temperatures (20°C–25°C) where, based on modeled responses to leaf temperature, g_{sref} would be underestimated and $\delta g_s/\delta \ln D$ would be overestimated. The net result of these two biases was that g_s predictions at 1.6 kPa in this temperature range were too low, reducing predicted C_i and A, and generating the Jarvis-Oren model's underestimation of seasonal carbon gain in AT trees. In contrast, the response of g_s to $\ln D$ was not well-captured by the Jarvis-Oren model for HT spruce at low leaf temperatures, as seen by the difference between measured and expected sensitivity at 10°C, leading to predictions of negative g_s at 10°C and 1.6 kPa (Figure 1e). However, the Jarvis-Oren model performed well at the warmer temperatures where HT leaves were operating (30°C–40°C). Because the Jarvis-Oren model predicted both HT g_{sref} and $\delta g_s/\delta \ln D$ well at leaf temperatures of 30°C–35°C, the model produced good closure of the carbon budget in this treatment.

[37] The Linear Optimization model predicted both AT and HT carbon gain well, consistent with the theory that stomata regulate g_s to maximize photosynthetic carbon gain while minimizing water loss [*Givnish and Vermeij*, 1976; *Cowan*, 1978; *Cowan and Farquhar*, 1977; *Hari et al.*, 1986; *Arneth et al.*, 2002; *Konrad et al.*, 2008; *Katul et al.*, 2009, 2010]. This and the Leuning model were the only models to accurately capture seasonal carbon gain within 10% of modeled costs in both treatments. The similarity in their success is not surprising, as the Linear Optimization model resembles the Leuning model except that their D reduction functions are not identical (see Appendix). And while the Leuning model generated instantaneous WUE values that most closely matched our measured values, instantaneous WUE in woody C_3 species varies from 1.0–7.8 μmol mmol^{-1} (with the highest value being for *Picea glauca*) [*Yoo et al.*, 2009] and from 2–10 μmol mmol^{-1} in our data, so only the Ball-Berry model produced WUE values outside our measured range. Our finding that the Leuning and Linear Optimization models both perform well contrasts with *Nijs et al.* [1997], who found that an approach based on a form of optimization performed more poorly than either the Ball-Berry or Leuning models in plants grown under both ambient and future CO_2 and temperature conditions. It should be emphasized that *Nijs et al.* [1997] evaluated a form of optimization theory based on maximizing instantaneous WUE, which is not comparable with the constant marginal water use efficiency used in the Linear Optimization model, although the two water use efficiencies

can be theoretically linked. As shown in the Appendix, the flux-based instantaneous WUE is not an intrinsic plant property, but varies with external environmental conditions. In the context of the Linear Optimization model, WUE increases linearly with increasing C_a and, perhaps more pertinent here, declines nonlinearly (as $D^{-1/2}$) with increasing D.

[38] The Linear Optimization model can explain g_s patterns in plants grown at different CO_2 concentrations and exposed to various water stress levels [*Katul et al.*, 2009, 2010; *Manzoni et al.*, 2011]. Our results add to the conclusion that this approach is useful for dealing with not only current vegetation, but also plants under future climate change scenarios. The Linear Optimization model uses a species-specific λ, which was held constant in both growth temperatures; the ability of this same λ to close the carbon budget for both treatments suggests that λ does not vary appreciably with warming. Other environmental conditions can alter λ: elevated CO_2 increases λ in a predictable way [*Katul et al.*, 2010; *Manzoni et al.*, 2011], but variations in λ with water availability are more complex. Soil volumetric water content between 15% and 30% had almost no effect on λ in Scots pine (*Pinus sylvestris*), and while decreasing soil water content can increase λ sevenfold, this only occurred at extremely stressful conditions [*Kolari et al.*, 2009]. Recent work has shown that λ varies with soil water availability, and that the shape of this response curve differs between plant functional types [*Manzoni et al.*, 2011]. While we found no need to vary λ between treatments, more research on the effect of growth temperature on λ is needed to make a definitive statement on whether λ will change with rising air temperatures.

5. Conclusions

[39] Large-scale modeling efforts, such as coupled vegetation-climate, hydrologic and ecological models, currently rely on semi-empirical g_s models. In fact, the Ball-Berry model was used in global climate models as early as 1995 [*Sellers et al.*, 1995], and more detailed biosphere-atmosphere models primarily employ the Ball-Berry formulation [*Baldocchi*, 1997; *Anderson et al.*, 2000; *Luo et al.*, 2001; *Reichstein et al.*, 2003; *Blanken and Black*, 2004] and Leuning models tested here [*Whitehead et al.*, 2001; *Keenan et al.*, 2010]. We show that the semi-empirical Leuning and the Linear Optimization-based models performed best for spruce grown at ambient and elevated temperatures, both in capturing measured g_s on a short time-scale and carbon gain on a longer, seasonal time-scale. Since optimization theory does not use a priori relationships between g_s and environmental conditions, but focuses on ecological theories to predict them, these models are likely to hold true across future conditions where empirical data is scarce. If a semi-empirical model is to be used in large-scale modeling, our results support the use of the Leuning model over the Ball-Berry model, particularly in vegetation modeled under future climate scenarios [see also *Nijs et al.*, 1997]. However, changing the Leuning model D reduction function from $1/(1 + D/D_o)$ to $D^{-1/2}$ is preferable, for its consistency with the *Oren et al.* [1999] function (tested across many scales and species) and the advantage of reducing the number of empirical parameters needed to model g_s. Evaluating the impact of this change on climate model outputs, particularly under future climates, would be a first step toward testing the robustness of current predictions of vegetation-climate feedbacks.

Appendix A: A Linearized Optimality Approach and Its Connection to the Leuning and Ball-Berry Models

[40] Linearizing the biochemical demand function in equation (1) results in a much simpler (and insightful) model for optimal g_s. The linearization requires the assumption that the variability of C_i only marginally affects the denominator of equation (1), leading to an approximation of $a_2 + C_i = a_2 + (C_i/C_a)C_a \approx a_2 + sC_a$. As a result,

$$A = \frac{a_1(C_i - \Gamma*)}{a_2 + sC_a}. \tag{A1}$$

It must be stressed here that only in the denominator of equation (A1), s is treated as a model constant. Combining this linearized photosynthesis model with equation (2) results in an expression for C_i and A given by:

$$C_i(g_s) = \frac{a_1\Gamma* + a_2C_ag_s + {C_a}^2g_s}{a_1 + a_2g_s + g_sC_as}, A(g_s) = \frac{a_1(C_a - \Gamma*)g_s}{a_1 + g_s(a_2 + sC_a)}. \tag{A2}$$

The objective function to be maximized by an autonomous leaf is to maximize photosynthesis for a given transpiration rate (E) resulting in:

$$f(g_s) = A - \lambda f_c = \frac{a_1(C_a - \Gamma*)g_s}{a_1 + g_s(a_2 + sC_a)} - \lambda a_c g_s D, \tag{A3}$$

and upon differentiating this objective function with respect to g_s, this yields:

$$\frac{\partial f(g_s)}{\partial g_s} = -a_c\lambda D + \frac{a_1^2\left(C_a - \Gamma^*\right)}{[a_1 + g_s(a_2 + sC_a)]^2}. \tag{A4}$$

Note that the convexity of $f(g_s)$ versus g_s ensures that a maximum exist that can be determined by setting $\partial f(g_s)/\partial g_s = 0$ (i.e., maximum carbon gain for a given water loss). Solving for g_s results in:

$$g_s = \frac{a_1}{a_2 + sC_a}\left(-1 + \sqrt{\frac{C_a - \Gamma^*}{a_c\lambda D}}\right). \tag{A5}$$

Apart from the compensation point, this expression is identical to the one derived by *Hari et al.* [1986]. With this optimal conductance, the photosynthesis is given as:

$$A = \frac{a_1\left(C_a - \Gamma^*\right)}{a_2 + sC_a}\left[1 - \sqrt{\frac{a_c\lambda D}{\left(C_a - \Gamma^*\right)}}\right]. \tag{A6}$$

The above expression can be rearranged to yield:

$$\frac{a_1}{a_2 + sC_a} = \frac{A}{(C_a - \Gamma*)}\frac{1}{\left[1 - \sqrt{\frac{a_c\lambda D}{(C_a - \Gamma*)}}\right]}, \tag{A7}$$

so that

$$g_s = \frac{A}{(C_a - \Gamma_*)} \frac{\left(-1 + \sqrt{\frac{C_a - \Gamma_*}{a_c \lambda D}}\right)}{\left[1 - \sqrt{\frac{a_c \lambda D}{(C_a - \Gamma_*)}}\right]} = \frac{A}{(C_a - \Gamma_*)} \sqrt{\frac{C_a - \Gamma_*}{a_c \lambda D}}. \quad \text{(A8)}$$

If $\lambda = \lambda_o C_a / C_o$, where λ_o and C_o are the intrinsic water use efficiency at the growth CO_2 concentration and the growth CO_2 concentration, respectively (such that the marginal water use efficiency increases linearly with increasing C_a), then

$$g_s = \frac{A}{(C_a - \Gamma_*)} \frac{\left(-1 + \sqrt{\frac{C_a - \Gamma_*}{a_c \lambda D}}\right)}{\left[1 - \sqrt{\frac{a_c \lambda D}{(C_a - \Gamma_*)}}\right]}$$

$$= \frac{A}{(C_a - \Gamma_*)} \sqrt{\frac{C_a(1 - \Gamma_*/C_a)}{a_c \lambda_o D C_a / C_o}} \approx m_2 \frac{A}{(C_a - \Gamma_*)} \frac{1}{D^{1/2}}. \quad \text{(A9)}$$

This functional form is identical to the Leuning model except that the vapor pressure deficit reduction function is $D^{-1/2}$ instead of $\left(1 + \frac{D}{D_o}\right)^{-1}$. Moreover, the sensitivity parameter of the Leuning model m_2 is given as $m_2 = \sqrt{\frac{C_o(1 - \Gamma_*/C_a)}{a_c \lambda_o}}$. Likewise, this Linear Optimization result is analogous to the Ball-Berry model if $D^{-1/2}$ is replaced by RH.

[41] Based on the Linear Optimization results, the instantaneous water-use efficiency (WUE) can also be related to λ_o, given as:

$$WUE = \frac{A}{E} \approx C_a \sqrt{\lambda_o / C_o} (a_c D)^{-1/2}. \quad \text{(A10)}$$

Note that if λ_o is constant, then WUE linearly increases with increasing C_a and nonlinearly decreases with increasing D. Hence, unlike the marginal water use efficiency, the flux-based water use efficiency is not an 'intrinsic' plant property and it does vary with external environmental conditions.

[42] It is also instructive to compare the canonical form of the optimality solution in equation A5 with analytical solutions to the Ball-Berry or the Leuning models when intercepts b_1 and b_2 are small compared to g_s. Upon combining equations (1) and (2) with equation (5), we obtain the following for the Ball-Berry model:

$$g_s \approx \frac{a_1 m_1 RH(-1 + RH)}{(\Gamma_* - c_a) + m_1 RH(a_2 + C_a)} \quad \text{(A11)}$$

$$A \approx \frac{a_1(-1 + RH)(c_a - \Gamma_*)}{(\Gamma_* - c_a) + m_1 RH(a_2 + C_a)}. \quad \text{(A12)}$$

Repeating the same analysis with equation (6) for the Leuning model, we obtain:

$$g_s \approx \frac{a_1 m_2 (1 + D/D_o)^{-1}\left(-1 + (1 + D/D_o)^{-1}\right)}{(\Gamma_* - c_a) + m_2 (1 + D/D_o)^{-1}(a_2 + C_a)} \quad \text{(A13)}$$

$$A \approx \frac{a_1\left(-1 + (1 + D/D_o)^{-1}\right)(c_a - \Gamma_*)}{(\Gamma_* - c_a) + m_2 (1 + D/D_o)^{-1}(a_2 + C_a)}. \quad \text{(A14)}$$

Naturally, the explicit dependence of g_s on the driving forces (RH and D), and thus temperature, differs across models. When comparing the models in Figures 5–7, the intercepts b_1 and b_2 were not ignored. While an analytical solution can be derived with intercepts b_1 and b_2 being finite, its mathematical form is too unwieldy for comparative purposes across models.

[43] **Acknowledgments.** We thank S. Manzoni, G. Vico, and S. Palmroth for feedback on earlier versions of this manuscript. Way, Katul, and Oren acknowledge support from the Natural Sciences and Engineering Research Council of Canada, the U.S. Department of Energy through the Office of Biological and Environmental Research (BER) Terrestrial Carbon Processes (TCP) program (FACE and NICCR grants DE-FG02-95ER62083, DE-FC02-06ER64156, and DE-SC000697), the National Science Foundation (NSF-AGS-1102227, NSF-EAR-10-13339, and NSF-CBET-103347), and the U.S. Department of Agriculture (2011-67003-30222).

References

Acosta M., M. Pavelka, R. Pokorny, D. Janous, and M. V. Marek (2008), Seasonal variation in CO_2 efflux of stems and branches of Norway spruce trees, *Ann. Bot. (Lond.)*, *101*, 469–477, doi:10.1093/aob/mcm304.

Ainsworth, E. A., and A. Rogers (2007), The response of photosynthesis and stomatal conductance to rising [CO_2]: Mechanisms and environmental interactions, *Plant Cell Environ.*, *30*, 258–270, doi:10.1111/j.1365-3040.2007.01641.x.

Anderson, M. C., J. M. Norman, T. P. Meyers, and G. R. Diak (2000), An analytical model for estimating canopy transpiration and canopy assimilation fluxes based on canopy light use efficiency, *Agric. For. Meteorol.*, *101*, 265–289, doi:10.1016/S0168-1923(99)00170-7.

Aphalo, P. J., and P. G. Jarvis (1991), Do stomata respond to relative humidity?, *Plant Cell Environ.*, *14*, 127–132, doi:10.1111/j.1365-3040.1991.tb01379.x.

Arneth, A., J. Lloyd, H. Santruckova, M. Bird, S. Grigoryev, Y. N. Kalaschnikov, G. Gleixner, and E. D. Schulze (2002), Response of central Siberian Scots pine to soil water deficit and long-term trends in atmospheric CO_2 concentration, *Global Biogeochem. Cycles*, *16*(1), 1005, doi:10.1029/2000GB001374.

Baldocchi, D. (1997), Measuring and modeling carbon dioxide and water vapour exchange over a temperate broad-leaved forest during the 1995 summer drought, *Plant Cell Environ.*, *20*, 1108–1122, doi:10.1046/j.1365-3040.1997.d01-147.x.

Baldocchi, D., and T. Meyers (1998), On using eco-physiological, micrometeorological and biogeochemical theory to evaluate carbon dioxide, water vapor and trace gas fluxes over vegetation: A perspective, *Agric. For. Meteorol.*, *90*, 1–25, doi:10.1016/S0168-1923(97)00072-5.

Ball, J. T., I. E. Woodrow, and J. A. Berry (1987), A model predicting stomatal conductance and its contribution to the control of photosynthesis under different environmental conditions, in *Progress in Photosynthesis Research, Proceedings of the VII International Congress on Photosynthesis*, vol. 4, edited by I. Biggins, pp. 221–224, Martinus Nijhoff, Dordrecht, Netherlands.

Betts, R. A., et al. (2007), Projected increase in continental runoff due to plant responses to increasing carbon dioxide, *Nature*, *448*, 1037–1041, doi:10.1038/nature06045.

Blanken, P. D., and T. A. Black (2004), The canopy conductance of a boreal aspen forest, Prince Albert National Park, Canada, *Hydrol. Processes*, *18*, 1561–1578, doi:10.1002/hyp.1406.

Buckley, T. N., K. A. Mott, and G. D. Farquhar (2003), A hydromechanical and biochemical model of stomatal conductance, *Plant Cell Environ.*, *26*, 1767–1785, doi:10.1046/j.1365-3040.2003.01094.x.

Campbell, G. S., and J. M. Norman (1998), *An Introduction to Environmental Biophysics*, Springer, Berlin.

Collatz, G. J., J. T. Ball, C. Grivet, and J. A. Berry (1991), Physiological and environmental-regulation of stomatal conductance, photosynthesis and transpiration: A model that includes a laminar boundary-layer, *Agric. For. Meteorol.*, *54*, 107–136, doi:10.1016/0168-1923(91)90002-8.

Cowan, I. R. (1978), Stomatal behaviour and environment, *Adv. Bot. Res.*, *4*, 117–228, doi:10.1016/S0065-2296(08)60370-5.

Cowan, I. R., and G. D. Farquhar (1977), Stomatal function in relation to leaf metabolism and environment, *Symp. Soc. Exp. Biol.*, *31*, 471–505.

Cowling, S. A., and R. F. Sage (1998), Interactive effects of low atmospheric CO_2 and elevated temperature on growth, photosynthesis and respiration in *Phaseolus vulgaris*, *Plant Cell Environ.*, *21*, 427–435, doi:10.1046/j.1365-3040.1998.00290.x.

Cox, P. M., R. A. Betts, C. D. Jones, S. A. Spall, and I. J. Totterdell (2000), Acceleration of global warming due to carbon-cycle feedbacks in a coupled climate model, *Nature*, *408*, 184–187, doi:10.1038/35041539.

Damour, G., T. Simonneau, H. Cochard, and L. Urban (2010), An overview of models of stomatal conductance at the leaf level, *Plant Cell Environ.*, *33*, 1419–1438.

Darwin, F. (1898), Observations on stomata, *Proc. R. Soc. London*, *63*, 413–417, doi:10.1098/rspl.1898.0053.

Day, M. E. (2000), Influence of temperature and leaf-to-air vapor pressure deficit on net photosynthesis and stomatal conductance in red spruce (*Picea rubens*), *Tree Physiol.*, *20*, 57–63.

Ellsworth, D. S., R. Oren, C. Huang, N. Phillips, and G. R. Hendrey (1995), Leaf and canopy responses to elevated CO_2 in a pine forest under free-air CO_2 enrichment, *Oecologia*, *104*, 139–146, doi:10.1007/BF00328578.

Farquhar, G. D., S. von Caemmerer, and J. A. Berry (1980), A biochemical model of photosynthetic CO_2 assimilation in leaves of C3 species, *Planta*, *149*, 78–90, doi:10.1007/BF00386231.

Fredeen, A. L., and R. F. Sage (1999), Temperature and humidity effects on branchlet gas-exchange in white spruce: An explanation for the increase in transpiration with branchlet temperature, *Trees Struct. Funct.*, *14*, 161–168, doi:10.1007/s004680050220.

Gedney, N., P. M. Cox, R. A. Betts, O. Boucher, C. Huntingford, and P. A. Stott (2006), Detection of a direct carbon dioxide effect in continental river runoff records, *Nature*, *439*, 835–838, doi:10.1038/nature04504.

Givnish, T. J., and G. J. Vermeij (1976), Sizes and shapes of liane leaves, *Am. Nat.*, *110*, 743–778, doi:10.1086/283101.

Hari, P., A. Makela, E. Korpilahti, and M. Holmberg (1986), Optimal control of gas exchange, *Tree Physiol.*, *2*, 169–176.

Heath, J. (1998), Stomata of trees growing in CO_2-enriched air show reduced sensitivity to vapor pressure deficit and drought, *Plant Cell Environ.*, *21*, 1077–1088, doi:10.1046/j.1365-3040.1998.00366.x.

Iivonen, S., S. Kaakinen, A. Jolkkonen, E. Vapaavuori, and S. Linder (2006), Influence of long-term nutrient optimization on biomass, carbon and nitrogen acquisition and allocation in Norway spruce, *Can. J. For. Res.*, *36*, 1563–1571, doi:10.1139/x06-035.

Jackson, R. B., C. W. Cook, J. S. Pippen, and S. M. Palmer (2009), Increased belowground biomass and soil CO_2 fluxes after a decade of carbon dioxide enrichment in a warm-temperate forest, *Ecology*, *90*, 3352–3366, doi:10.1890/08-1609.1.

Jarvis, P. G. (1976), The interpretation of the variations in leaf water potential and stomatal conductance found in canopies in the field, *Philos. Trans. R. Soc. London, Ser. B*, *273*, 593–610, doi:10.1098/rstb.1976.0035.

Jordan, D. B., and W. L. Ogren (1981), Species variation in the specificity of ribulose carboxylase/oxygenase, *Nature*, *291*, 513–515, doi:10.1038/291513a0.

Jordan, D. B., and W. L. Ogren (1984), The CO_2/O_2 specificity of ribulose 1,5-bisphosphate carboxylase oxygenase–dependence on ribulose bisphosphate concentration, pH and temperature, *Planta*, *161*, 308–313, doi:10.1007/BF00398720.

Juang, J. Y., G. G. Katul, M. B. Siqueira, P. C. Stoy, and H. R. McCarthy (2008), Investigating a hierarchy of Eulerian closure models for scalar transfer inside forested canopies, *Boundary Layer Meteorol.*, *128*, 1–32, doi:10.1007/s10546-008-9273-2.

Kaakinen, S., R. Pilspanen, S. Lehto, J. Metsometsa, U. Nilsson, P. Saranpaa, S. Linder, and E. Vapaavuori (2009), Growth, wood chemistry, and fibre length of Norway spruce in a long-term nutrient optimization experiment, *Can. J. For. Res.*, *39*, 410–419, doi:10.1139/X08-180.

Katul, G. G., D. Ellsworth, and C. T. Lai (2000), Modeling assimilation and intercellular CO_2 from measured conductance: A synthesis of approaches, *Plant Cell Environ.*, *23*, 1313–1328, doi:10.1046/j.1365-3040.2000.00641.x.

Katul, G. G., S. Palmroth, and R. Oren (2009), Leaf stomatal responses to vapour pressure deficit under current and CO_2-enriched atmosphere explained by the economics of gas exchange, *Plant Cell Environ.*, *32*, 968–979, doi:10.1111/j.1365-3040.2009.01977.x.

Katul, G., S. Manzoni, S. Palmroth, and R. Oren (2010), A stomatal optimization theory to describe the effects of atmospheric CO_2 on leaf photosynthesis and transpiration, *Ann. Bot. (Lond.)*, *105*, 431–442, doi:10.1093/aob/mcp292.

Keenan, T., S. Sabate, and C. Gracia (2010), Soil water stress and coupled photosynthesis-conductance models: Bridging the gap between conflicting reports on the relative roles of stomatal, mesophyll conductance, and biochemical limitations to photosynthesis, *Agric. For. Meteorol.*, *150*, 443–453, doi:10.1016/j.agrformet.2010.01.008.

Kemp, P. R., and G. J. Williams (1980), A physiological basis for niche separation between *Agropyron smithii* (C3) and *Bouteloua gracilis* (C4), *Ecology*, *61*, 846–858, doi:10.2307/1936755.

Kim, H.-S., R. Oren, and T. M. Hinkley (2008), Actual and potential transpiration and carbon assimilation in an irrigated poplar plantation, *Tree Physiol.*, *28*, 559–577.

Kolari, P., E. Nikinmaa, and P. Hari (2009), Vegetation processes: Photosynthesis and drought, in *Boreal Forest and Climate Change*, *Adv. Global Change Res.*, vol. 34, edited by P. Hari and S. Kulmala, pp. 256–262, Springer, New York.

Konrad, W., A. Roth-Nebelsick, and M. Grein (2008), Modelling of stomatal density response to atmospheric CO_2, *J. Theor. Biol.*, *253*, 638–658, doi:10.1016/j.jtbi.2008.03.032.

Kostiainen, K., S. Kaakinen, P. Saranpaa, B. D. Sigurdsson, S. O. Lundqvist, S. Linder, and E. Vapaavuori (2009), Stem wood properties of mature Norway spruce after 3 years of continuous exposure to elevated [CO_2] and temperature, *Global Change Biol.*, *15*, 368–379, doi:10.1111/j.1365-2486.2008.01755.x.

Kubien, D. S., and R. F. Sage (2008), The temperature response of photosynthesis in tobacco with reduced amounts of Rubisco, *Plant Cell Environ.*, *31*, 407–418, doi:10.1111/j.1365-3040.2008.01778.x.

Kumagai, T., G. G. Katul, A. Porporato, S. Saitoh, M. Ohashi, T. Ichie, and M. Suzuki (2004), Carbon and water cycling in a Bornean tropical rainforest under current and future climate scenarios, *Adv. Water Resour.*, *27*, 1135–1150, doi:10.1016/j.advwatres.2004.10.002.

Lai, C. T., G. Katul, R. Oren, D. Ellsworth, and K. Schäfer (2000), Modeling CO_2 and water vapor turbulent flux distributions within a forest canopy, *J. Geophys. Res.*, *105*, 26,333–26,351, doi:10.1029/2000JD900468.

Leuning, R. (1995), A critical-appraisal of a combined stomatal-photosynthesis model for C_3 plants, *Plant Cell Environ.*, *18*, 339–355, doi:10.1111/j.1365-3040.1995.tb00370.x.

Luo, Y., B. Medlyn, D. Hui, D. Ellsworth, J. Reynolds, and G. Katul (2001), Gross primary productivity in Duke Forest: Modeling synthesis of CO_2 experiment and eddy-flux data, *Ecol. Appl.*, *11*, 239–252.

Manzoni, S., G. Vico, G. Katul, P. A. Fay, H. W. Polley, S. Palmroth, and A. Porporato (2011), Optimizing stomatal conductance for maximum carbon gain under water stress: A meta-analysis across plant functional types and climates, *Funct. Ecol.*, *25*, 456–467, doi:10.1111/j.1365-2435.2010.01822.x.

Medlyn, B. E., et al. (2001), Stomatal conductance of forest species after long-term exposure to elevated CO_2 concentration: A synthesis, *New Phytol.*, *149*, 247–264, doi:10.1046/j.1469-8137.2001.00028.x.

Meidner, H. (1987), Three hundred years of research on stomata, in *Stomatal Function*, edited by E. Zeigler, G. D. Farquhar, and I. R. Cowan, pp. 7–28, Stanford Univ. Press, Palo Alto, Calif.

Monson, R. K., M. A. Stidham, G. J. Williams, G. E. Edwards, and E. G. Uribe (1982), Temperature-dependence of photosynthesis in *Agropyron smithii* Rydb. 1. Factors affecting net CO_2 uptake in intact leaves and contribution from Ribulose-1,5-bisphosphate carboxylase measured in vivo and in vitro, *Plant Physiol.*, *69*, 921–928, doi:10.1104/pp.69.4.921.

Mortazavi, B., J. P. Chanton, J. L. Prater, A. C. Oishi, R. Oren, and G. Katul (2005), Temporal variability in C-13 of respired CO_2 in a pine and a hardwood forest subject to similar climatic conditions, *Oecologia*, *142*, 57–69, doi:10.1007/s00442-004-1692-2.

Mott, K. A., and D. Peak (2010), Stomatal responses to humidity and temperature in darkness, *Plant Cell Environ.*, *33*, 1084–1090.

Ng, P. A. P., and P. G. Jarvis (1980), Hysteresis in the response of stomatal conductance in *Pinus sylvestris* L. needles to light: Observations and a hypothesis, *Plant Cell Environ.*, *3*, 207–216.

Niinemets, U. (1997), Energy requirements for foliage construction depends on tree size in young *Picea abies* trees, *Trees Struct. Funct.*, *11*, 420–431.

Nijs, I., R. Ferris, H. Blum, G. Hendrey, and I. Impens (1997), Stomatal regulation in a changing climate: A field study using Free Air Temperature Increase (FATI) and Free Air CO_2 Enrichment (FACE), *Plant Cell Environ.*, *20*, 1041–1050, doi:10.1111/j.1365-3040.1997.tb00680.x.

Norman, J. M. (1982), Simulation of microclimates, in *Biometeorology and Integrated Pest Management*, edited by J. L. Hatfield and I. Thompson, pp. 65–99, Academic, New York.

Oren, R., J. S. Sperry, G. G. Katul, D. E. Pataki, B. E. Ewers, N. Phillips, and K. V. R. Schäfer (1999), Survey and synthesis of intra- and interspecific variation in stomatal sensitivity to vapour pressure deficit, *Plant Cell Environ.*, *22*, 1515–1526, doi:10.1046/j.1365-3040.1999.00513.x.

Peak, D., and K. A. Mott (2011), A new, vapour-phase mechanism for stomatal responses to humidity and temperature, *Plant Cell Environ.*, *34*, 162–178, doi:10.1111/j.1365-3040.2010.02234.x.

Pieruschka, R., G. Huber, and J. A. Berry (2010), Control of transpiration by radiation, *Proc. Natl. Acad. Sci. U. S. A.*, *107*, 13,372–13,377, doi:10.1073/pnas.0913177107.

Rayment, M. B., D. Loustau, and P. G. Jarvis (2000), Measuring and modeling conductances at three organizational scales: Shoot, branch and canopy, *Tree Physiol.*, *20*, 713–723.

Reichstein M., J. Tenhunen, O. Roupsard, J.-M. Ourcival, S. Rambal, F. Miglietta, A. Peressotti, M. Pecchiari, G. Tirone, and R. Valentini (2003), Inverse modeling of seasonal drought effects on canopy CO_2/H_2O exchange in three Mediterranean ecosystems, *J. Geophys. Res.*, *108*(D23), 4726, doi:10.1029/2003JD003430.

Sage, R. F., and T. D. Sharkey (1987), The effect of temperature on the occurrence of O_2 and CO_2 insensitive photosynthesis in field-grown plants, *Plant Physiol.*, *84*, 658–664, doi:10.1104/pp.84.3.658.

Sage, R. F., D. A. Way, and D. S. Kubien (2008), Rubisco, Rubisco activase and global climate change, *J. Exp. Bot.*, *59*, 1581–1595, doi:10.1093/jxb/ern053.

Santrucek, J., and R. F. Sage (1996), Acclimation of stomatal conductance to a CO_2-enriched atmosphere and elevated temperature in *Chenopodium album*, *Aust. J. Plant Physiol.*, *23*, 467–478, doi:10.1071/PP9960467.

Scarth, G. W. (1927), Stomatal movement: Its regulation and regulatory role: A review, *Protoplasma*, *2*, 498–511, doi:10.1007/BF01604752.

Schäfer, K. V., R. Oren, C. T. Lai, and G. G. Katul (2002), Hydrologic balance in an intact temperate forest ecosystem under ambient and elevated atmospheric CO_2 concentration, *Global Change Biol.*, *8*, 895–911, doi:10.1046/j.1365-2486.2002.00513.x.

Sellers, P. J., et al. (1995), Remote-sensing of the land surface for studies of global change: Models, algorithms, experiments, *Remote Sens. Environ.*, *51*, 3–26, doi:10.1016/0034-4257(94)00061-Q.

Sellers, P. J., et al. (1996), Comparison of radiative and physiological effects of doubled atmospheric CO_2 on climate, *Science*, *271*, 1402–1406, doi:10.1126/science.271.5254.1402.

Silim, S. N., N. Ryan, and D. S. Kubien (2010), Temperature responses of photosynthesis and respiration in *Populus balsamifera* L.: Acclimation versus adaptation, *Photosynth. Res.*, *104*, 19–30, doi:10.1007/s11120-010-9527-y.

Siqueira, M., and G. Katul (2002), Estimating heat sources and fluxes in thermally stratified canopy flows using higher-order closure models, *Boundary Layer Meteorol.*, *103*, 125–142, doi:10.1023/A:1014526305879.

Tjoelker, M. G., J. Oleksyn, and P. B. Reich (1999), Acclimation of respiration to temperature and CO_2 in seedlings of boreal tree species in relation to plant size and relative growth rate, *Global Change Biol.*, *5*, 679–691, doi:10.1046/j.1365-2486.1999.00257.x.

von Caemmerer, S., and P. Quick (2000), Rubisco: Physiology in vivo, in *Advances in Photosynthesis: Physiology and Metabolism*, edited by R. C. Leegood, T. D. Sharkey, and S. von Caemmerer, pp. 86–107, Kluwer Acad., Dordrecht, Netherlands.

Wang, B. S. P., and P. Berjak (2000), Beneficial effects of moist chilling on the seeds of black spruce (*Picea mariana* [Mill.] B.S.P.), *Ann. Bot. (Lond.)*, *86*, 29–36, doi:10.1006/anbo.2000.1150.

Watts, W. R., and R. E. Neilson (1978), Photosynthesis in Sitka spruce (*Picea sitchensis* (Bong.) Carr.) 8. Measurements of stomatal conductance and $^{14}CO_2$ uptake in controlled environments, *J. Appl. Ecol.*, *15*, 245–255, doi:10.2307/2402934.

Way, D. A., and R. Oren (2010), Differential responses to increased growth temperatures between trees from different functional groups and biomes: A review and synthesis of data, *Tree Physiol.*, *30*, 669–688, doi:10.1093/treephys/tpq015.

Way, D. A., and R. F. Sage (2008a), Elevated growth temperatures reduce the carbon gain of black spruce (*Picea mariana* (Mill.) B.S.P.), *Global Change Biol.*, *14*, 624–636, doi:10.1111/j.1365-2486.2007.01513.x.

Way, D. A., and R. F. Sage (2008b), Thermal acclimation of photosynthesis in black spruce (*Picea mariana* (Mill.) B.S.P.), *Plant Cell Environ.*, *31*, 1250–1262, doi:10.1111/j.1365-3040.2008.01842.x.

Weston, D. J., and W. L. Bauerle (2007), Inhibition and acclimation of C_3 photosynthesis to moderate heat: A perspective from thermally contrasting genotypes of *Acer rubrum* (red maple), *Tree Physiol.*, *27*, 1083–1092.

Whitehead, D., J. R. Leathwick, and A. S. Walcroft (2001), Modeling annual carbon uptake for the indigenous forests of New Zealand, *For. Sci. [Washington D. C.]*, *47*, 9–20.

Wong, S. C., and F. X. Dunin (1987), Photosynthesis and transpiration of trees in a Eucalypt forest stand–CO_2, light and humidity responses, *Aust. J. Plant Physiol.*, *14*, 619–632, doi:10.1071/PP9870619.

Wong, S. C., I. R. Cowan, and G. D. Farquhar (1979), Stomatal conductance correlates with photosynthetic capacity, *Nature*, *282*, 424–426, doi:10.1038/282424a0.

Wullschleger, S. D., C. A. Gunderson, P. J. Hanson, K. B. Wilson, and R. J. Norby (2002), Sensitivity of stomatal and canopy conductance to elevated CO_2 concentration–interacting variables and perspectives of scale, *New Phytol.*, *153*, 485–496, doi:10.1046/j.0028-646X.2001.00333.x.

Yamori, W., K. Noguchi, Y. T. Hanba, and I. Terashima (2006), Effects of internal conductance on the temperature dependence of the photosynthetic rate in spinach leaves from contrasting growth temperatures, *Plant Cell Physiol.*, *47*, 1069–1080, doi:10.1093/pcp/pcj077.

Yoo, C. Y., H. E. Pence, P. M. Hasegawa, and M. V. Mickelbart (2009), Regulation of transpiration to improve crop water use, *Crit. Rev. Plant Sci.*, *28*, 410–431, doi:10.1080/07352680903173175.

G. G. Katul, H.-S. Kim, R. Oren, and D. A. Way, Nicholas School of the Environment, Duke University, Box 90328, Durham, NC 27708, USA. (danielle.way@duke.edu)